Advanced Journal of Chemistry-Section B
Natural Products and Medical Chemistry

Journal homepage: http://www.ajchem-b.com/

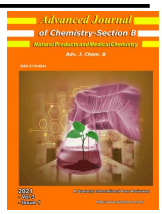

Original Research Article

Crystal structure, Hirshfeld surface, Energy framework and Molecular docking analysis of 4-(methoxyphenyl)acetic acid

Ruchika Sharma[1], Sumati Anthal[1], Nitin G. Ghatpande[2,3], Mahidansha M. Shaikh[2,3], Jagannath S. Jadhav[4], Saminathan Murugavel[5], Sonachalam Sundramoorthy[6] and Rajni Kant[1*]

[1]*Chemical Crystallography Laboratory, Department of Physics, University of Jammu, Jammu Tawi-180006, India.*
[2]*Department of pharmaceutical Chemistry, School of Health Science, University of KwaZulu-Natal, Durban-4041, South Africa.*
[3]*Unique Med Chem Laboratories, L-64, Chincholli MIDC, Solapur-413255, M. S., India.*
[4]*Department of Chemistry, Shivaji University, Kolhapur-416004, M.S., India.*
[5]*Department of Physics, Thanthai Periyar Government Institute of Technology, Vellore- 632002, Tamil Nadu, India.*
[6]*Department of Physics, Agni College of Technology OMR, Thalambur, Chennai-600130, Tamil Nadu, India.*

ARTICLE INFO

Article history

Submitted: 2021-10-01
Revised: 2021-11-24
Accepted: 2021-12-01
Available online: 2021-12-16
Manuscript ID: AJCB-2110-1097
DOI: 10.22034/ajcb.2021.307316.1097

KEYWORDS

Acetic acid,
Crystallography,
Hydrogen bond,
Energy frameworks,
Dimer

ABSTRACT

The crystal structure of (4-methoxyphenyl) acetic acid ($C_9H_{10}O_3$) exists in the monoclinic space group $P2_1/c$ having unit cell parameters: a = 16.268 (15), b = 5.858 (5), c = 9.157 (8) Å, β = 95.24 (2)°, and Z = 4. The structure has been solved by X-ray diffraction methods and it converges to a final reliability index of 0.0620 for 1117 observed reflections. Two intermolecular hydrogen bonds of the type C-H....O and O-H....O have been observed. The O-H....O hydrogen bond leads to the formation of a dimer with R_2^2 (8) graph set motif and it is found linked to another C-H....O intermolecular hydrogen bond. The molecule has been characterized for Hirshfeld surface, energy frameworks and molecular docking studies. The Hirshfeld surface (HS) analysis was performed for the identification of all the close contacts and their strength in the crystal structure. The energy frameworks were analyzed to examine the molecular stability and also to ascertain the dominant energy component. The molecular docking investigations lead to the finding that (4-methoxyphenyl)acetic acid may act as an active anti-microbial (antibacterial and antifungal) drug.

HIGHLIGHTS

- Synthesis, single crystal X-ray structure and Hirshfeld surfaces (HS) of (4-methoxy phenyl)acetic acid have been reported.
- The results as accrued form the HS and 2D Fingreprint plots were examined in the light of intermolecular interactions, their strength and possible contribution in the molecular structure of the difunctional compound with carboxylate and electron rich methoxy functionalities. The interaction energies between molecular pairs were investigated and assessed through energy framework modules.
- The molecule of (4-methoxy phenyl) acetic acid was docked with DNA gyrase and Lanosterol 14 α-demethylase was selected as target for the antifungal agent. The molecular docking method validates the anti-microbial (antibacterial and antifungal) activity of the investigated molecule.

* Corresponding author: Rajni Kant
✉ E-mail: rkant.ju@gmail.com
☏ Tel number: +91 191 2432051

GRAPHICAL ABSTRACT

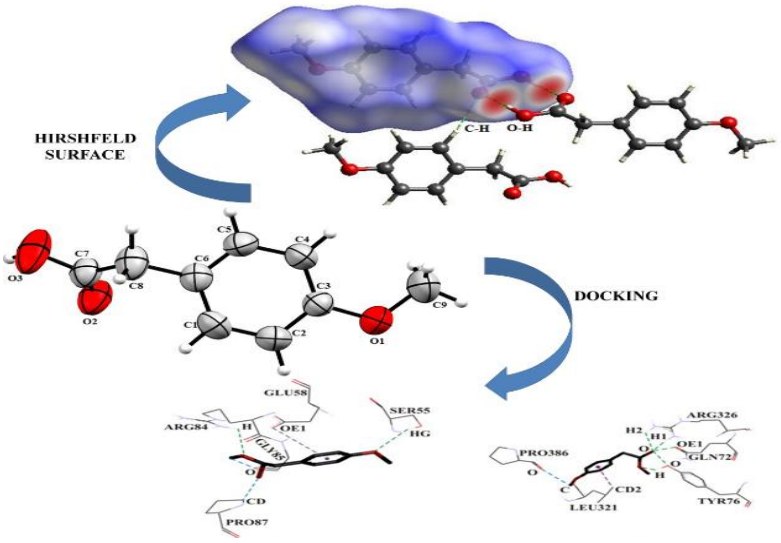

1.Introduction

Phenylacetic acid belongs to an important class of organic compounds that show a wide range of biological applications. The title compound, (4-methoxyphenyl)acetic acid (4MPAA), is a monocarboxylic acid, also known a difunctional compound with carboxylate and electron rich methoxy functionalities (commonly known as homoanisic acid) [1]. It is used as an intermediate for pharmaceuticals and other organic synthesis and has also been reported to inhibit the germination of cress and lettuce seeds [1]. It has many applications in various synthesis, for example, in the synthesis of heterocyclic compounds [2] and in the synthesis of nonopioid antitussive agent Dextromethorphan [3]. Herein, we report its crystal structure in continuation of our study towards the synthesis of N-Acyl/aroyl spiro[chromane-2,4-piperidin]-4(3H)-one, wherein we used the title compound as a key substrate.

In view of some interesting activities exhibited by phenylacetic acid derivatives [4-7], we got interested in determining its X-ray crystal structure and some other related properties, Hirshfeld surface, Energy frameworks and Molecular docking. The Hirshfeld surface (HS) analysis helps determine the nature and characteristics of intermolecular interactions which influence the molecular packing in crystals [8]. The energy framework analysis helps obtain the magnitude of interaction energies in the crystal structure [9-11]. The Crystal Explorer (17.5) software has been used for the calculation of Hirshfeld surface and energy frameworks [12].

Molecular docking analysis has been carried out to predict the biological activity of 4MPAA using drug discovery systems [13]. DNA gyrase perform a significant part in biosynthesis of bacterial circular DNA. The obstructing of DNA gyrase causes bacterial death [14]. Owing to this reason we have selected DNA gyrase enzyme as a target for antibacterial agent. Hence 4MPAA was docked with DNA gyrase (PDB Id: 3G75) [15]. The blocking of Lanosterol 14 α-demethylase resists the production of ergosterol

in fungi. Most of the fungal growth cannot be possible without ergosterol [16]. Due to this reason Lanosterol 14 α-demethylase was select as target for antifungal agent. Hence 4MPAA was docked with Lanosterol 14 α-demethylase (PDB Id: 1EA1) [17]. Further, the docking results of 4MPAA were compared with standard drugs ciprofloxacin (Bacteria) and fluconazole (fungi). The present work is a part of our ongoing investigations on the synthesis and crystallographic analysis of some medicinally important organic (small) molecules containing acetic acid as a substituent [18-20].

2. Experimental

2.1 Synthesis and crystallization

The material was obtained commercially (Spectrochem Ltd) and was dissolved in toluene at 70°C. The solution was filtered upon cooling and the filtrate yielded nice crystals of (4-methoxyphenyl) acetic acid at room temperature (slow evaporation) over a week. The chemical structure is shown in Figure 1.

2.2 X-ray structure elucidation

A well-defined single crystal of 4MPAA (having size: 0.40x0.30x0.20 mm) was used for intensity data collection. The diffraction data were measured (Φ - ω scan mode) at 293 K on D8 Venture Bruker diffractometer using MoKα radiation (λ = 0.71073 Å). The data were collected in an angular range of 2.51 - 25.98°.

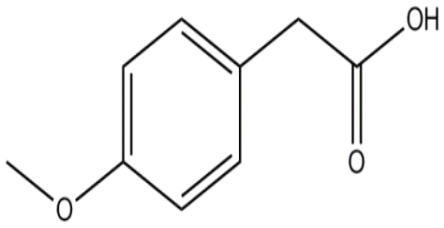

Fig. 1: Chemical diagram of 4-(methoxyphenyl)acetic acid (m.p. 84-86°C).

A total of 20687 reflections were measured of which 1707 were found independent and 1117 were treated as observed (limiting criteria used is I > 2σ (I)). SHELXS97 software [22] was used for generating the model structure and refinement of the same was performed using SHELXL97 [22]. The final cycle of least - squares refinement yielded a final R-factor 0.062 (*w*R (F^2) = 0.1773) for 1117 observed reflections. The non-hydrogen atoms were obtained from the best E-map.

The minimum and maximum electron density is -0.26 and 0.23 e $Å^{-3}$, respectively, and the scattering factors were picked up from International Tables for X-ray Crystallography (1995, Vol. C, Tables 4.2.6.8 and 6.1.1.4) [23]. MERCURY [24] software was used for determining various structural parameters like bond distances, bond angles, torsion angles while PLATON [25] and PARST [26] software provided information about the molecular interactions. A summary of the crystal data is presented in Table 1 and some selected bond geometric parameters in Table 2.

2.3 Computational details

The atomic coordinates were imported from the validated CIF to Crystal Explorer (17.5) [12] and the HS plots of 4MPAA were generated. The energy framework investigations were performed using Crystal Explorer (17.5) with B3LYP function and 6-31G (d, p) basis set. AutoDock Vina software [27] was employed using a suite of automated docking tools (ADT).

3. RESULTS AND DISCUSSION

3.1 X-ray of 4-(methoxyphenyl)acetic acid

An ORTEP view of the 4MPAA molecule indicating the atom numbering scheme is shown in Figure 2.

Table 1. Precise crystal data for 4MPAA

CCDC number	**2093980**
Molecular formula	$C_9H_{10}O_3$
Molecular weight	166.17
Crystal system	Monoclinic
Space group	$P2_1/c$
Data collection temperature	293(K)
***a*, *b*, *c* (Å)**	16.268 (2), 5.858 (5), 9.157 (8)
α, β, γ (°)	95.24 (2)
V (Å^3)	869.0 (1)
Z	4
Wavelength (Mo*Kα*)	0.71073 Å
Absorption	0.095 (mm^{-1})
R_{int}	0.082, 0.616
h, k, l	-20 to 20, -7 to 7, -11 to 11
Final R-factor	0.0620
Weighted R-factor	0.1773
GOOF	1.050
No. of measured, independent and observed reflections	20687, 1707, 1117
No. of parameters	111

The bond distances in the benzene ring lie between 1.372 (4) Å and 1.393 (4) Å and this indicates its aromatic character. The methoxy group is coplanar with the benzene ring (dihedral angle being 4.09 (2)°) while the carboxylic acid shows some deviation from the plane of benzene ring (dihedral angle being 67.48 (2)°). The carbon-oxygen bond distances [C7-O3 =1.305 (4) Å, C7-O2 = 1.201 (4) Å and C3-O1 = 1.372 (3) Å] are in agreement with some analogous structures [28, 29]. The endocyclic bond angle C5-C6-C1 is significantly less than its normal value and it may be due to the presence of carboxylic group at C6. The presence of $-OCH_3$ group at C3 causes the endo and exo-cyclic bond angles around C3 to deviate from the normal values. The bond C6-C8 exhibits substantial torsion (73.0(4)°) with respect to the phenyl and carboxylic acid moieties.

The structure is stabilized by O-H….O and C-H….O intermolecular interactions (Table 3). The O3-H3….O2 intermolecular bond results in the formation of a dimer (R_2^2 (8) graph- set motif) which is further connected to the C5-H5….O2 hydrogen bond (Figure 3). This feature has also been observed in the crystal structure of (3-methoxyphenyl) acetic acid [30]. The unit cell packing of 4MPAA is shown in Figure 4 [Mercury, (24)].

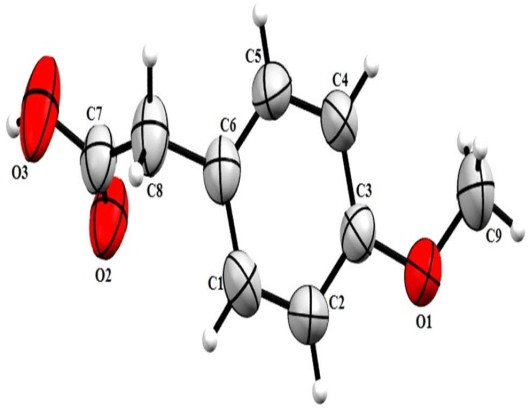

Fig. 2: ORTEP view of 4-(methoxyphenyl)acetic acid (Thermal ellipsoids drawn at 50 % probability level).

3.2 Hirshfeld surface and 2D fingerprint plot analysis

Hirshfeld surface analysis provides an idea of packing modes, molecular surface and the intrinsic interactions responsible for the packing of molecules in the crystal. It is a quantitative way to study the intermolecular

Interactions present in a crystal structure. The Hirshfeld surfaces and fingerprint plots were mapped using Crystal Explorer (17.5) software [12]. The B3LYP/6-31G (d, p) basis set using TONTO [31] (Crystal Explorer (17.5) software) gives the Hirshfeld surface volume (212.26 $Å^3$) and surface area volume (211.47 $Å^2$) of the structure.

Figure 5 depicts the Hirshfeld surface projected over the normalised contact distance (d_{norm}) which is calculated using the following equation

$$d_{norm} = \frac{di - r^{iv}}{r^{iv}} + \frac{de - r^{ev}}{r^{ev}}$$

where d_i is the distance from a point on the surface to the nearest nucleus inside the surface, d_e is the distance from a point on the surface to the nearest nucleus outside the surface and r^{iv} is the van der Waal's radii of the atoms internal to the surface, r^{ev} is the van der Waal's radii of the atoms external to the surface. The value of d_{norm} may be positive or negative depending on whether the intermolecular interactions are shorter or longer than the van der Waal's radii [32].

The HS mapping shows regions with three colours: red, blue and white. The bright red spots are due to the presence of strong O3-H3…O2 contacts. The red and blue regions represent interactions which are respectively shorter and longer than the Vander Waals radii while the white colour region represents the contacts equal to the van der Waals radii (with d_{norm} =0) [32].

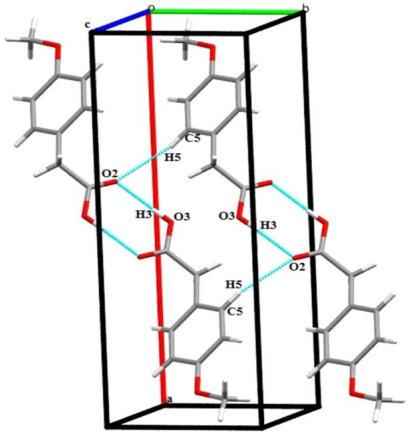

Fig. 3: Unit cell plot showing $R_2^2(8)$ dimer ring

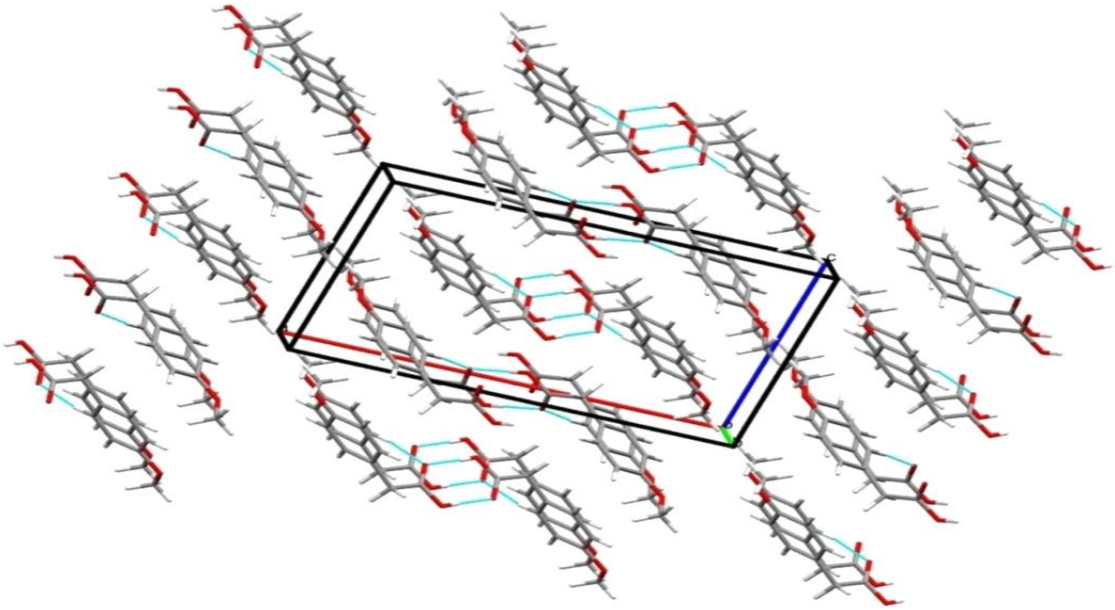

Fig. 4: Unit cell molecular packing (b-axis).

Table 2. Some selected bond geometric parameters

Bond Distance(Å)		Bond Distance(Å)	
O1— C3	1.372(3)	O1— C9	1.418(4)
O2—C7	1.201(4)	C2—C1	1.372(4)
C2—C1	1.372(4)	C3—C4	1.377(4)
O3-C7	1.305(4)	C6—C8	1.503(4)
C3—C4	1.377(4)	C7—C8	1.505(5)
O3—C7	1.305(4)		
Bond Angle(°)		**Bond Angle(°)**	
C3—O1—C9	118.0(2)	O1—C3—C2	116.5(2)
O1—C3—C4	124.8(3)	C5—C6—C8	121.3(3)
C4—C3—C2	118.7(3)	C4—C5—C6	122.3(3)
C5—C6—C1	116.6(3)	O2—C7—O3	122.4(3)
C1—C6—C8	122.1(3)	O3—C7—C8	113.2(3)
C2—C1—C6	121.9(3)	C6—C8—C7	115.3(2)
O2—C7—C8	124.5(3)		
Torsion Angle(°)		**Torsion Angle(°)**	
C9—O1—C3—C4	4.0(4)	C1—C6—C8—C7	73.0(4)
C5—C6—C8—C7	108.5(4)	O3—C7—C8—C6	-167.6(3)
O2—C7—C8—C6	11.8(5)		

Table 3. D-H...A intermolecular bonds (Å, °).

D–H...A	D–H	H...A	D...A	D–H...A
O3–H3···O2^{i}	0.82	1.87	2.687(5)	178
C5–H5···O2^{ii}	2.52	2.52	3.434(5)	167

Symmetry codes: (i) 1-x, 2-y, 1-z (ii) x, -1+y, z

The fingerprint plots as shown in Figure 6 were generated with d_{norm} range lying between -0.7030 - 1.2241 Å, respectively. For any specified pairs of d_i and de, the white colour indicates poor occurrence of contacts, blue shows some and the green colour represents better frequency of occurrence of intermolecular contacts. The spikes which occur in the extended form, as shown in Figure 6(b), are due to O-H/H-O contacts while the ones as shown in Figure 6(c) and 6(d) occur due to H-H and C-H/H-C intermolecular contacts.

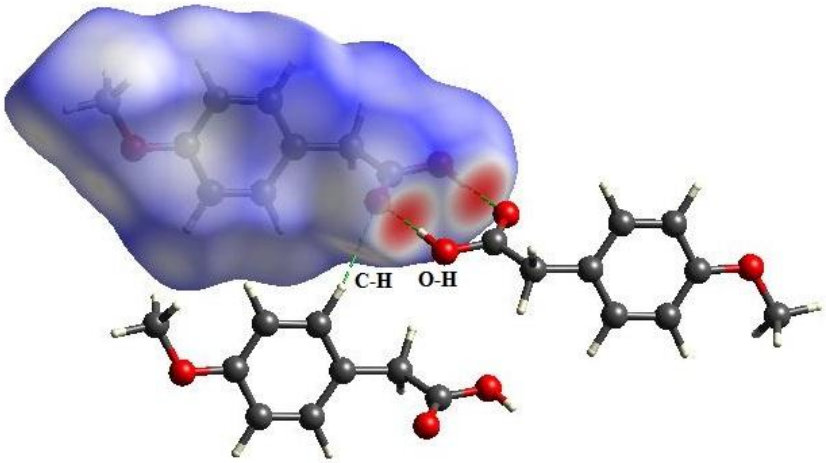

Fig. 5: Hirshfeld Surface as mapped over d_{norm}.

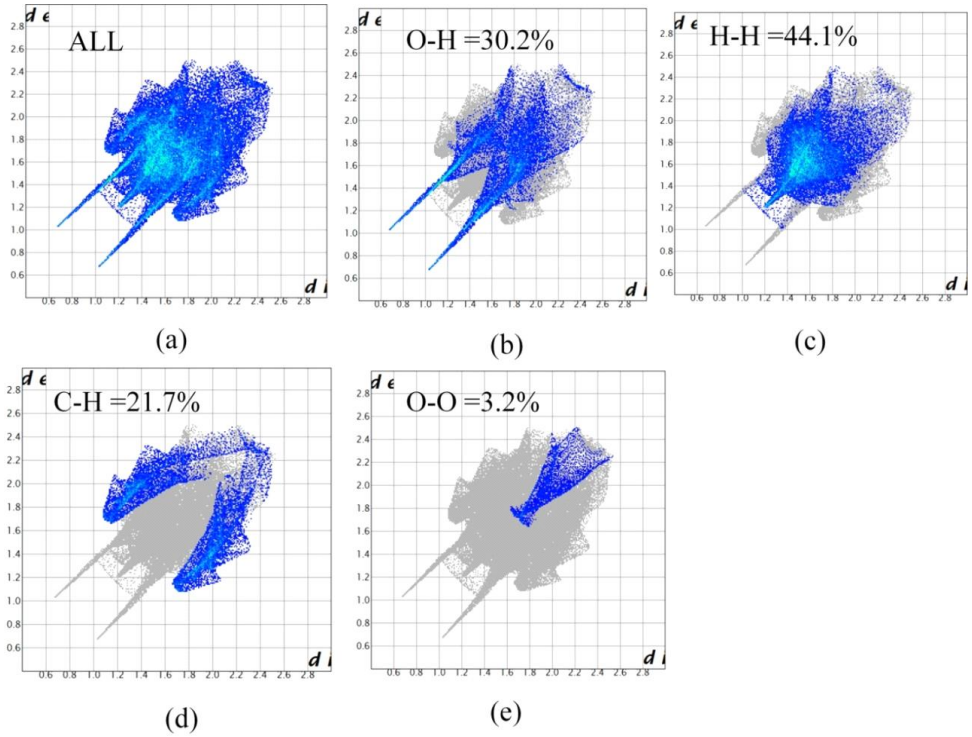

Fig. 6: Fingerprint plots of intermolecular contacts.

3.2.1 Electrostatic potential, Shape index and Curvedness

In order to have some insights about the kind and role of intermolecular interactions, the B3LYP/6-31G (d, p) basis set was used for the mapping of electrostatic potential [33]. The electropositive area near O3-H3 atoms is complementary to the electronegative region around O2 atom (Figure 7(a)). The Hirshfeld surface indicates the existence of complementary pairs of red and blue regions which show the areas of touching points of two molecular Hirshfeld surfaces (Figure 7(b)) [31]. The red region on the shape index indicates the cluster of the surface around the acceptor atoms, while the surface around the donor atoms is highlighted as blue bumps region. The π-π interaction in (4-methoxyphenyl)acetic acid is non-existent as there are no adjacent red and blue triangles on the surface. Curvedness, a function which is the root mean square curvature of the surface [31], mapped onto the surface of 4MPAA shows large green regions, segregated by dark blue curves [Figure 7(c)]. The planar stacking between the molecules is missing due to the absence of flat patches on the surface.

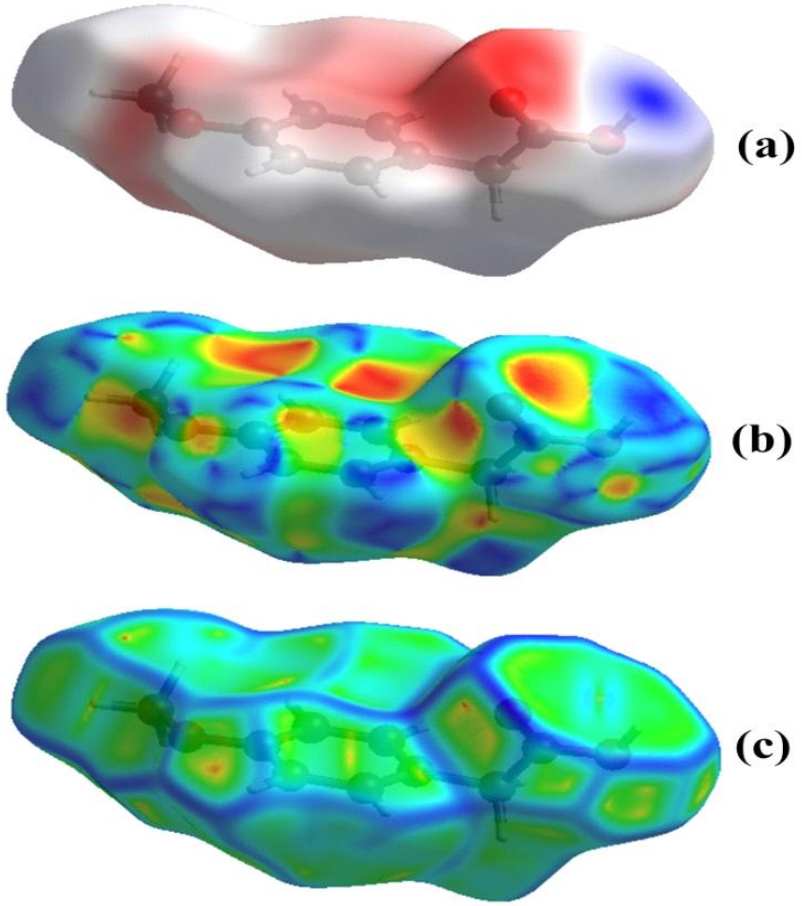

Fig. 7: (a) Electrostatic potential map (b) Shape index plot mapped over Hirshfeld surface (c) Curvedness, mapped onto the surface, showing the non- planar stacking of the molecules.

3.3 Energy frameworks

The crystallographic information file (crystal geometry and hydrogen bond distances) was used as input to Crystal Explorer 17.5 software and the intermolecular interaction energies were calculated for the energy-framework analysis. The energy framework calculations, being indicative of supramolecular construction of molecules in the crystal [34, 35], were obtained by employing B3LYP/6-31G (d, p) functional basis set, where a group of molecules were generated within a radius of 3.8 Å around a single molecule. The neighbouring molecules (density matrices) are generated within this shell by applying crystallographic symmetry operations with respect to the central molecule (density matrix). The calculated interaction energies are presented in Table 4. The molecular pair-wise interaction energies, calculated for the construction of energy frameworks, were used to evaluate the net interaction energies. The scale factors for benchmarked energies used for the construction of energy models for B3LYP/6-311G (d, p) electron densities (k_ele = 1.057, k_pol = 0.740, k_disp = 0.871, k_rep = 0.618) [35] help compute corresponding interaction energies which are E_ele = -139.5 kJ/mol, E_pol = -34.4 kJ/mol, E_dis = -108 kJ/mol and E_rep = 184 kJ/mol, respectively. The total interaction energy is -153.2 kJ/mol. Thus, it becomes evident that the electrostatic interaction energy dominates the dispersion energy framework.

Table 4. Different interaction energies of the molecules pairs in kJ/mol.

	N	Symop	R	Electron Density	E_ele	E_pol	E_dis	E_rep	E_tot
	1	-x, -y, -z	12.53	B3LYP/6-31G(d,p)	1.1	-0.2	-3.3	0.9	-1.3
	2	-x, y+1/2, -z+1/2	9.15	B3LYP/6-31G(d,p)	-1.4	-0.4	-7.0	2.4	-6.4
	1	-x, -y, -z	10.56	B3LYP/6-31G(d,p)	-9.2	-1.4	-9.1	9.4	-12.9
	2	x, -y+1/2, z+1/2	6.00	B3LYP/6-31G(d,p)	-6.6	-1.1	-22.0	13.9	-18.3
	2	x, y, z	5.86	B3LYP/6-31G(d,p)	-8.5	-2.4	-16.1	13.7	-16.3
	2	x, -y+1/2, z+1/2	4.99	B3LYP/6-31G(d,p)	-5.7	-2.9	-23.7	12.6	-21.1
	1	-x, -y, -z	7.88	B3LYP/6-31G(d,p)	3.8	-0.8	-10.9	3.1	-4.1
	2	-x, y+1/2, -z+1/2	10.22	B3LYP/6-31G(d,p)	-0.8	-0.3	-3.5	0.5	-3.8
	1	-x, -y, -z	9.23	B3LYP/6-31G(d,p)	-112.2	-24.9	-12.4	127.5	-69.0

The visualization of some of these interaction energies i.e., coulomb (red), dispersion (green) and total energy (blue) along the three respective crystallographic axes is presented in Figure 8. In the energy framework, an overall scale factor is employed to expand or contract the size of the cylinders [9]. The cylinders shown therein give the relative strength of the molecular packing in different directions. The absence of cylinders in a particular direction is due to the exclusion of few interactions below a certain threshold energy value and such (weak) interactions are generally avoided to make the figures look less crowded.

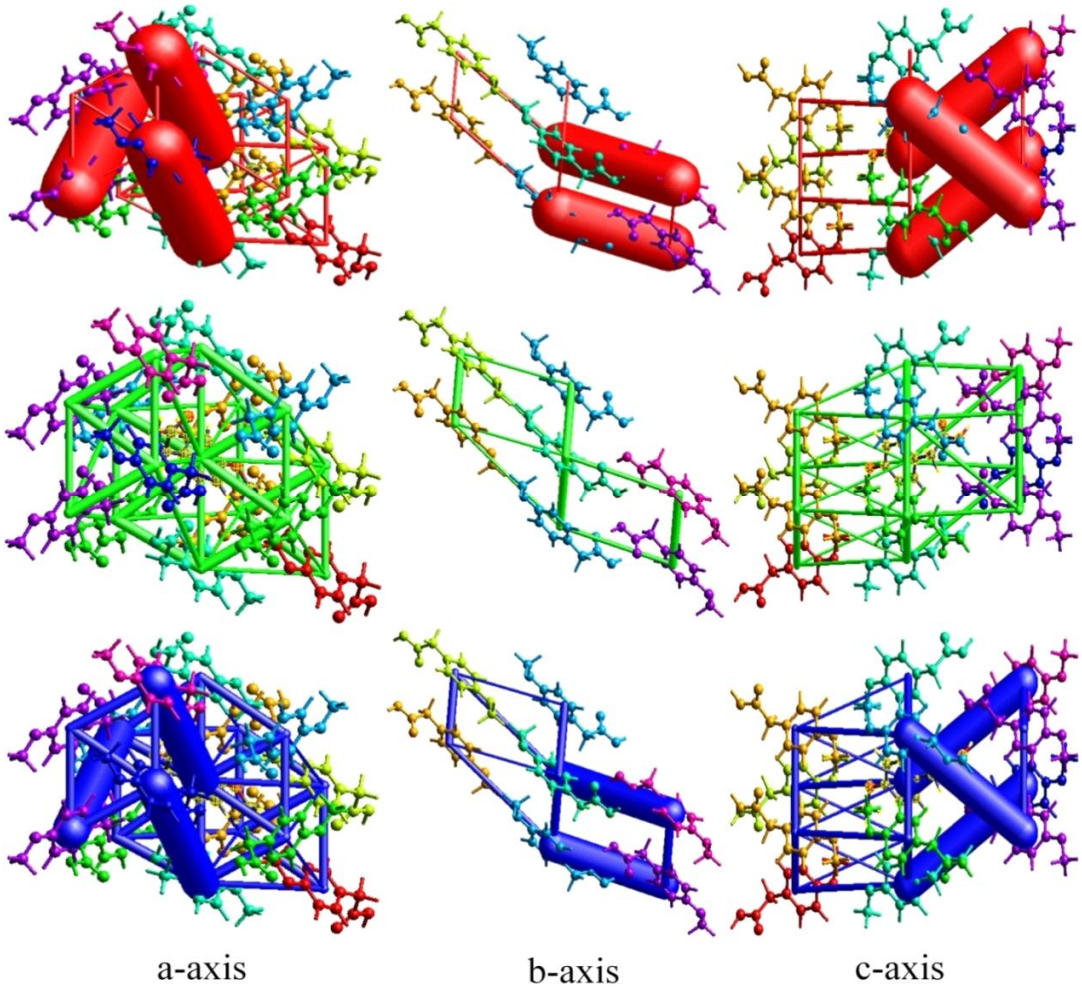

Fig. 8: The graphical representation of coulomb interaction energy (red), dispersion energy (green) and total interaction energy (blue) of the molecule along a, b and c-axis.

3.4 Molecular docking analysis

The target protein DNA gyrase and enzyme Lanosterol 14 α-demethylase were imported from the protein data bank (www.rcsb.org/pdb). The grid center was pinpointed at X= 51.20, Y = -3.99, Z = 17.94 (for DNA gyrase) and X = -17.29, Y = -7.28, Z = 63.72 (for lanosterol-14α-demethylase). Discovery Studio Visualizer [16] was used to model and visualize the stabilized complex structures. 4MPAA - DNA gyrase complex was stabilized by hydrogen interactions with residue SER55, ARG84, PRO87 and GLY85 and electrostatic interaction with residue GLU58 (Fig 9(a)). The binding energy, bond length and bonding type of interaction in 4MPAA - DNA gyrase complex are listed in Table 5. The docking result shows that binding energy of 4MPAA - DNA gyrase complex (-5.7 kcal m^{-1}) is higher as compared with Ciprofloxacin-DNA gyrase complex (-4.01 kcal m^{-1}) [36].

The 4MPAA - lanosterol-14α-demethylase complex is stabilized by hydrogen interactions with residue TVR76, ARG326, GLN72 and PRO386 and hydrophobic interaction with residue LEU321 (Fig 9(b)). The binding energy, bond length and bonding type of interaction in

lanosterol-14α-demethylase complex are also listed in Table 5. The binding energy of 4MPAA - lanosterol-14α-demethylase complex (-5.7 kcal m^{-1}) comes out to be better when compared with Fluconazole - lanosterol-14α-demethylase complex (-3.59 kcal m^{-1}) [36].

As obvious from Table 5, 4MPAA exhibits strong affinity with the targets (DNA gyrase / lanosterol-14α-demethylase) and possesses more docking energy than the standard drugs (Ciprofloxacin and Fluconazole). Hence, 4MPAA may act as an active anti-microbial (antibacterial and antifungal) drug.

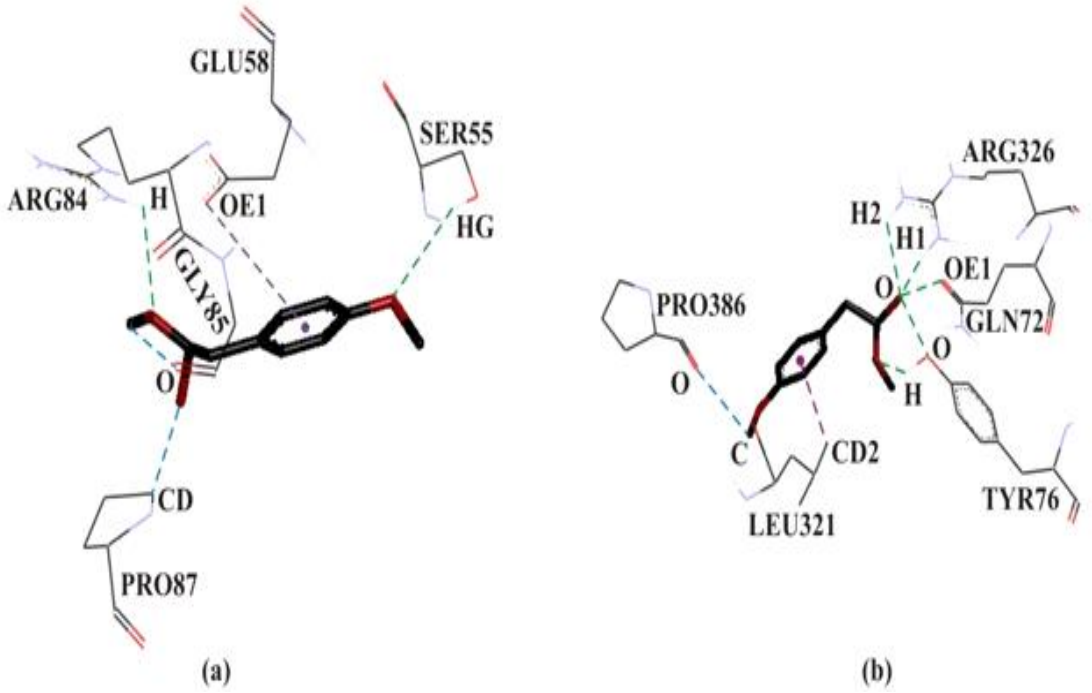

Fig. 9: Molecular interaction of (4-methoxyphenyl)acetic acid with (a) DNA gyrase and (b) Lanosterol 14 α- demethylase binding site.

4. CONCLUSIONS

In order to examine the nature and characteristics of intermolecular interactions which influence the molecular docking and the magnitude and role of interaction energies, we have carried out the synthesis and X-ray crystallography of (4-methoxyphenyl)acetic acid. The single crystal X-ray structure analysis shows the presence of two intermolecular hydrogen interactions. The O3-H3...O2 hydrogen interaction is responsible for the formation of a dimer (with R_2^2 (8) graph- set motif) which is further connected to the C5-H5...O2 intermolecular hydrogen bond. The Hirshfeld surface was analyzed to have an assessment about the molecular surface and intrinsic interactions responsible for the packing of molecules in the crystal structure of (4-methoxyphenyl)acetic acid. The 2D fingerprint plot analysis shows that the contribution of H-H contacts is maximum (44.1%). The shape index and curvedness plots as mapped over the Hirshfeld surface reveals that the π-π interaction is non-existent and the planar stacking between the molecules is also absent.

Table 5. Binding energy, hydrogen bonds of (4-methoxyphenyl)acetic acid with DNA gyrase and lanosterol-14-demethylase.

Complex*	Binding Energy (kcal m^{-1})	Interactions	Distance (Å)	Bonding	Bonding Types
1	**5.7**	SER55[HG…O]	2.9237	Hydrogen	H-bond
		ARG84[H…O]	2.6950	Hydrogen	H-bond
		PRO87[CD…O]	3.6463	Hydrogen	CH-bond
		[C…O]GLY85	3.6951	Hydrogen	CH-bond
		[π…OE1]GLU58	4.4668	Electrostatic	π-Anion
2	**5.7**	TVR76[H…O]	2.6018	Hydrogen	H-bond
		ARG326[H1…O]	2.0845	Hydrogen	H-bond
		ARG326[H2…O]	2.6835	Hydrogen	H-bond
		[O…OE1]GLN72	3.3113	Hydrogen	H-bond
		[O…OH]TYR76	3.1906	Hydrogen	H-bond
		[C…O]PRO386	3.7434	Hydrogen	CH-bond
		LEU321 [CD2…]	3.9644	Hydrophobic	π-σ

*1 = (4-methoxyphenyl)acetic acid + DNA gyrase
2= (4-methoxyphenyl)acetic acid + lanosterol-14-demethylase

To understand the molecular packing in the crystal via energy frameworks, the results indicate that the electrostatic interaction energy is quite dominant. The molecular docking results show that the binding energy of (4-methoxyphenyl)acetic acid - DNA gyrase complex (-5.7 kcal m^{-1}) is more as compared to Ciprofloxacin-DNA gyrase complex (-4.01 kcal m^{-1}) and the same is true in case of the binding energy of (4-methoxyphenyl)acetic acid - lanosterol-14-demethylase complex (-5.7 kcal m^{-1}) when compared with that of Fluconazole-lanosterol-14-demethylase complex (-3.59 kcal m^{-1}). This observation demonstrates that (4-methoxyphenyl)acetic acid may act as an active anti-microbial (antibacterial and antifungal) drug

Acknowledgement:
Rajni Kant is thankful to University of Jammu for some partial research grants released under RUSA 2.0 Project of Ministry of Human Resource Development, Government of India.

REFERENCES

[1] National Center for Biotechnology Information. PubChem Compound

Summary for CID 7690, 4 – Methoxyphenyl acetic acid. https://pubchem.ncbi.nlm.nih.gov/compound/4-Methoxyphenylacetic-acid, 2021.

[2] P.P. Deshpande, V.B. Nanduri, A. Pullockaran, H. Christie, R.H. Mueller and R.N. Patel, Microbial hydroxylation of *o*-bromophenylacetic acid: synthesis of 4-substituted-2,3-dihydrobenzofurans. *Journal of Industrial Microbiology and Biotechnol*ogy, 35 (2008) 901-906.

[3] T. Kumaraguru and N.W. Fadnavis, An Improved Process for the Preparation of (+)-3- Methoxy-N-formylmorphinan. *Organic Process Research & Development*, 18 (2014) 174-178.

[4] G. Tuncel and C. Nergiz, Antimicrobial effect of some olive phenols in a laboratory medium. *Letters in Applied Microbiology*, 17 (1993) 300-302.

[5] M.M. Alam and S.R. Adapa, A Facile Synthesis of Phenylacetic Acids via Willgerodt-Kindler Reaction Under PTC Condition. *Synthetic Communications*, 33 (2003) 59-63.

[6] J. Baumann, F. Von Bruchhausen and G. Wurm, A structure-activity study on the influence of phenolic compounds and bioflavonoids on rat renal prostaglandin synthetase. *Naunyn-Schmiedeberg's Archives of Pharmacology,* 307 (1979) 73-78.

[7] K.V. Chamberlain and R.L. Wain, Studies on plant growth-regulating substances: XXXIII. The influence of ring substituents on the plant growth-regulating activity of phenylacetic acid. *Annals of Applied Biol*ogy, 69 (1971) 65-72.

[8] A.S. Mitchell, Novel tools for visualizing and exploring intermolecular interactions in molecular crystals. *Acta Crystallographica B,* 60 (2004) 627-668.

[9] M.J. Turner, S.P. Thomas, M.W. Shi, D. Jayatilaka and M.A. Spackman, Energy frameworks: insights into interaction anisotropy and the mechanical properties of molecular crystals. *Chemical Communications*, 51 (2015) 3735-3738.

[10] S.M. Kumar, B.N. Lakshminarayana, S. Nagaraju, S.S. Ananda, B.C. Manjunath, N.K. Lokanath and K. Byrappa, 3D energy frameworks of a potential nutraceutical. *Journal of Molecular Structure*, 1173 (2018) 300-306.

[11] S.M. Kumar, A.K. Kudva, B.C. Manjunath, P. Naveen, T. Prashanth, S.A. Khanum, N.K. Lokanath and P. Nagendra, 3D energy framework of a benzophenone acidic dimer. *Chemical Data Collections,* 19 (2019) 100168.

[12] M.J. Turner, J.J. Mckinnon, S.K. Wolff, D.J. Grimwood, P.R. Spackman, D. Jayatilaka and M.A. Spackman, Crystal Explorer 17, The University of Western Australia (2017).

[13] T. Lengauer and M. Rarey, Computational methods for biomolecular docking. *Current Opinion in Structural Biology*. 6 (3) (1996) 402-406.

[14] A. Wehenkel, P. Fernandez, M. Bellinzoni, V. Catherinot, N. Barilone, G. Labesse,M. Jackson and P.M. Alzari, The structure of PknB in complex with mitoxantrone, an ATP-competitive inhibitor, suggests a mode of protein kinase regulation in mycobacteria. *FEBS Letters,* 580 (2006) 3018-3022.

[15] N. Aoumeur, N. Tchouar, S. Belaidi, M. Ouassaf, T. Lanez and S. Chtita, Molecular docking studies for the identifications of

novel antimicrobial compounds targeting of staphylococcus aureus. *Moroccan Journal of Chemistry*, 9(2) (2021) 274-289.

[16] S.M. El-Feky, L.A. Abou-Zeid, M.A. Massoud, S.G. Shokralla1 and H.M. Eisa, Computational Design, Molecular Modeling and Synthesis of New 1,2,4 – Triazole Analogs with Potential Antifungal Activities. *SMU Medical Journal*, 1(2) (2014) 224-242.

[17] T. Jorda and S. Puig, Regulation of Ergosterol Biosynthesis in Saccharomyces cerevisiae. *Genes,* 11 (2020) 795.

[18] N.A. Wani, V.K. Gupta, R. Kant, S. Aravinda and R. Rai, Conformation and crystal structures of 1-aminocyclohexaneacetic acid (β 3,3 Ac 6 c) in N-protected derivatives. *Acta Crystallographica*, E70 (2014) 272-277.

[19] N.A. Wani, V.K. Gupta, R. Kant, S. Aravinda and R. Rai, 2-(1-Amino-4-tert-butylcyclohexyl)acetic acid (tBu-$\beta^{3,3}$-Ac_6c)hemihydrates. *Acta Crystallographica*, E69 (2013) o888.

[20] R. Kant, V.K. Gupta, K. Kapoor and B. Narayana, 2-(2-Chlorophenyl)acetic acid. *Acta Crystallographica Section E*, 68 (2012) o1940.

[21] G.M. Sheldrick, A Short History of SHELX. *Acta Crystallographica,* A64, (2008) 112-122.

[22] G.M. Sheldrick, *SHELXT* – Integrated space-group and crystal-structure determination. *Acta Crystallographica,* C71 (2015) 3-8.

[23] A.J.C. Wilson, International Tables for Crystallography Volume C: Mathematical, Physical and Chemical Tables. *Acta Crystallographica, A51 (1995) 441-444.*

[24] C.F. Macrae, I.J. Bruno, J.A. Chisholm, P.R. Edgington, P. McCabe, E. Pidcock, L. Rodriguez-Monge, R. Taylor, J. Van De Streek, and P.A. Wood, New Features for the Visualization and Investigation of Crystal Structures. *Journal of Applied* Crystallography, 41 (2008) 466-470.

[25] A.L. Spek, Structure validation in chemical crystallography. *Acta Crystallographica,* D65 (2009) 148-155.

[26] M. Nardelli, PARST: a system of Fortran routines for calculating molecular structure parameters from the results of crystal structure analyses. *Journal of Applied* Crystallography, 28 (1995) 659-659.

[27] O. Trott and A.J. Olson, AutoDock Vina: improving the speed and accuracy of docking with a new scoring function, efficient optimization and multithreading. *Journal of Computational Chemistry*, 31 (2010) 455-461.

[28] G.S. Khan, N.H. Rama, G. Qadeer, A. Noor, and R. Kempe, Crystal structure of methyl2-(2-formyl-3,4,5-trimethoxyphenyl)acetate, $C_{13}H_{16}O_6$. *Zeitschrift für Kristallographie – New Crystal Structures,* 221 (2006) 497-498.

[29] I.A. Guzei, A.R. Gunderson and N.J. Hill, 2-(3-Bromo-4-methoxyphenyl) acetic acid. *Acta Crystallographica,* E66 (2010) o1555-o1556.

[30] A.R. Choudhury and T.N. Guru Row, (3-Methoxyphenyl)acetic acid. *Acta Crystallographica,* E58 (2002) o889-o890.

[31] M.A. Spackman, and D. Jayatilaka, Hirshfeld surface analysis. *CrystEngComm*, 11 (2009) 19-32.

[32] J.J. McKinnon, D. Jayatilaka and M.A. Spackman, Towards quantitative analysis of intermolecular interactions with Hirshfeld surfaces. *Chemical Communications*, 37 (2007) 3814-3816.

[33] M.J. Turner, S. Grabowsky, D. Jayatilaka and M.A. Spackman, Accurate and Efficient Model Energies for Exploring Intermolecular Interactions in Molecular Crystals. *The Journal of Physical Chemistry Letters*, 5 (2014) 4249-4255.

[34] A.J. Edwards, C.F. Mackenzie, P.R. Spackman, D. Jayatilaka and M.A. Spackman, Intermolecular interactions in molecular crystals: what's in a name?. *Faraday Discussions,* 203 (2017) 93-112.

[35] C.F. Mackenzie, P.R. Spackman, D. Jayatilaka, and M.A. Spackman, CrystalExplorer model energies and energy frameworks: extension to metal coordination compounds, organic salts, solvates and open-shell systems. *IUCrJ,* 4 (2017) 575-587.

[36] S. Murugavel, S. Sundramoorthy, D. Lakshmanan, R. Subashini, P. Pavan Kumar, Synthesis, crystal structure analysis, spectral (NMR, FT-IR, FT-Raman and UV-Vis) investigations, molecular docking studies, antimicrobial studies and quantum chemical calculations of a novel 4-chloro-8-methoxyquinoline-2(1H)-one: an effective antimicrobial agent and an inhibition of DNA gyrase and lanosterol-14α-demethylase enzymes. *Journal of molecular structure*, 1131 (2017) 51-72.

HOW TO CITE THIS ARTICLE

Ruchika Sharma, Sumati Anthal, Nitin G. Ghatpande, Mahidansha M. Shaikh, Jagannath S. Jadhav, Saminathan Murugavel, Sonachalam Sundramoorthy and Rajni Kant, Crystal structure, Hirshfeld surface, Energy framework and Molecular docking analysis of 4-(methoxyphenyl)acetic acid, , Ad. J. Chem. B, 3 (2021) 333-347

DOI: 10.22034/ajcb.2021.307316.1097

URL: http://www.ajchem-b.com/article_141864.html